第5回地震時保有耐力法に基づく橋梁の耐震設計
に関するシンポジウム講演論文集 (2002年1月)

APPLICATION OF A 3D POUNDING MODEL FOR SEISMIC ANALYSIS ON ELEVATED BRIDGES

Ping ZHU [1], Masato ABE[2], Yozo FUJINO[3]

[1]Ph. D. Research fellow, zhu@bridge.t.u-tokyo.ac.jp
[2]Member, Associate Professor, masato@bridge.t.u-tokyo.ac.jp
[3]Fellow, Professor, fujino@bridge.t.u-tokyo.ac.jp

Department of Civil Engineering, University of Tokyo 7-3-1 Hongo, Bunkyo-Ku, Tokyo 113-8656, Japan

1. Introduction

Unseating of bridge girders/decks during earthquakes is very harmful to the safety and serviceability of bridges. Evidence from recent earthquake shows that pounding between bridge girders is one of the reasons lead to unseating. To conduct precise analysis, 3D modeling for both bridge structures and the pounding effects is needed. This paper presents the application of 3D modeling for elevated bridges considering poundings between girders. A three-span steel bridge was chosen for a case study. Pounding effects and countermeasures of pounding are discussed upon analysis results.

2. A 3D contact-friction model for pounding [1]

The problem considered herein is a general case of pounding by two bridge girders. As shown in Fig. 1, two girders contact with each other arbitrarily. They are referred to as contactor body and target body where a contact happens between contactor node and target surface. A 3D contact-friction model for the problem is illustrated in Fig. 2. The target surface is assumed as a rigid plane, which has not to be a rectangle. Vector **n** is the outer normal vector of the target surface. Node k is the contactor node at the contactor body, which penetrates into the target surface during contact. Point p is the physical contact point at the target surface.

The model utilizes material penetrations to compute forces during contact. Upon contact, a universal spring K_{cnt} between node k and point p is created to compute the force of contact. Two dashpots, C and C_t, are also applied to node k for simulating energy loss during contact. The contact force at node k, $\mathbf{F_k}$, can be computed as $\mathbf{F_k} = K_{cnt} \cdot \Delta_\mathbf{k}$ and be divided into normal and tangent components ($\mathbf{F_k}|_\mathbf{n}$ and $\mathbf{F_k}|_\mathbf{t}$ respectively), where vector **n** is the outer normal vector of the target surface and vector **t** is a projection vector of $\mathbf{F_k}$ to the target surface. During contact, status can be divided into stick contact and slide contact which can be decided by the ratio of tangent component of the contact force $|\mathbf{F_k}|_\mathbf{t}|$ to the normal one $|\mathbf{F_k}|_\mathbf{n}|$. Contact forces can be calculated separately for stick and slide conditions.

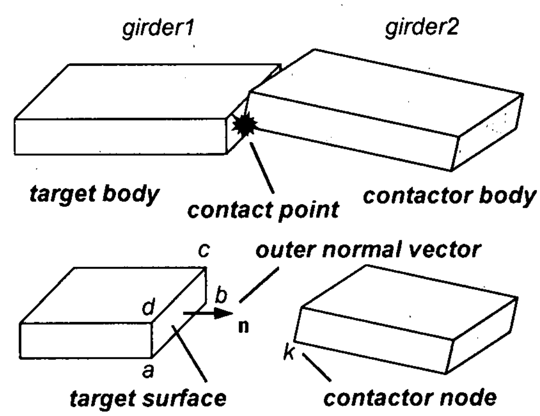

Fig. 1 Bridge girders in arbitrary contact

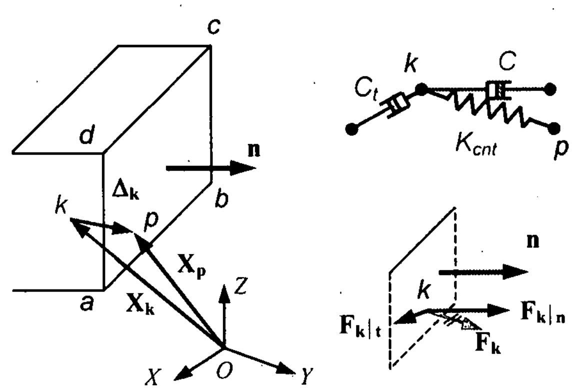

Fig. 2 Illustrations of the 3D contact-friction model

3. 3D modeling of elevated bridges

An elevated bridge is composed of foundations, piers and superstructures. Superstructures include supports, girders and decks. To conduct a precise analysis, detailed models for each of these components are needed. Considering steel elevated bridges isolated both in longitudinal and transversal directions, a bi-axial model of rubber bearing is adopted for supports[2]. The fiber model, known as a discretized-section model for nonlinear analysis, is used to model piers in the analysis. A bilinear hysteresis model is employed for fibers of steel. Soil-structure interactions should also be taken into account. A soil-grouped pile model with simplifications has been adopted[3]. This model uses a single equivalent beam instead of a group of piles. The cap stiffness of the single equivalent beam is calculated in frequency domain. Equivalent stiffness parameters, M, K, C, are fitted from the results.

4. Computation of a three-span steel bridge

A general-purpose dynamic analysis program for bridges has been developed. At the beginning of the development, a related work of 3D analysis for highway bridge structures from Tseng and Penzien[4] was referred. Written in C++, the program implements 3D models of bridge structures including the proposed pounding model. A typical three-span steel bridge has been selected for analysis. As shown in Fig. 3, fiber model is adopted at the first segment of each pier from foundation. Base-isolation rubber bearings are applied for each pier. For computation of pounding, a simple supported girder in each span is assumed. Restrainers are adopted as a countermeasure for pounding effects.

Computing conditions and parameters

Computations were conducted in three cases: 1) without pounding, 2) considering pounding and 3) considering pounding and applying restrainers. All parameters and the bridge structure model are the same for these three cases, except that in the third case, restrainers were adopted. In the first case of without pounding, no material contacts were assumed, though girders may overlap each other in a real case. Takatori waves from the 1995 Kobe earthquake were used as earthquake excitations in three-dimensional. Parameters for time-history analysis are as follow:

Time interval=0.001 (sec), duration=10 (sec). Data output at each 0.005 (sec).

Results and analyses

One node, node A, was picked from the center of girders of the mid span. Displacements for all the cases and accelerations for case2 and case3 were selected to output in longitudinal, transversal and rotating directions. Rotating direction is in a plane parallel to the ground. Results of computations are given in Fig. 4 and Fig. 5, which show comparisons of displacements and accelerations at node A. Responses of pounding at the middle span and side span show same trends. Longitudinal displacements are reduced according to poundings, while displacements at transversal do not have much change, as there is no face-to-face pounding assumed in this direction. A remarkable increase of rotating angle of the girder can be seen as a result of pounding. Results of accelerations show that the structure experiences strong reaction forces during pounding. And poundings, as complex reactions between girders, happen in a continuous manner with a start of a contact. Comparisons of displacement results for case2 and case3 show that the application of restrainers can reduce the pounding effecting dramatically, not only in the longitudinal direction, but also in the rotational direction. As a view of acceleration results, which refer to the forces induced by pounding, restrainers can also work effectively to reduce pounding forces.

5. Conclusions

This paper presents 3D modeling for analyses of elevated bridges under earthquakes including poundings between girders. A 3D contact-friction model for pounding between bridge girders has been adopted. Computations of a chosen three-span steel bridge considering arbitrary poundings between girders and a countermeasure with restrainers have been conducted. Results show: 1) poundings between girders may induce a remarkable increase of rotating angle to each girder; 2) restrainers can reduce pounding effects both in longitudinal and rotational directions.

6. Reference

1) Zhu P., Abe, M. and Fujino, Y. A 3D Contact-friction Model for Pounding at Bridges during Earthquakes, *Proceedings of The First M.I.T. Conference on Computational Fluid and Solid Mechanics*, Cambridge, Massachusetts, USA, 2001.
2) Abe M. Yoshida J, and Fujino Y. Uni-axial and Bi-axial Property of Base-Isolation Bearings and its Modeling (in Japanese). *Journal of Structural Mechanic sand Earthquake Engineering, JSCE*, 2002.
3) Konagai K. Shaking table test allowing interpretation of damage to structure in terms of energy influx and efflux through soil-structure interface. *Report of Research Project 1999 Grant-in-aid for Scientific Research (B) (No. 10450174)*, The Ministry of Education, Science, Sports and Culture, Japan.
4) Tseng WS and Penzien J. *Analytical Investigations of the Seismic Response of Long Multiple Span Highway Bridges*; EERC 73-12, Earthquake Engineering Research Center, University of California, Berkley, 1973.

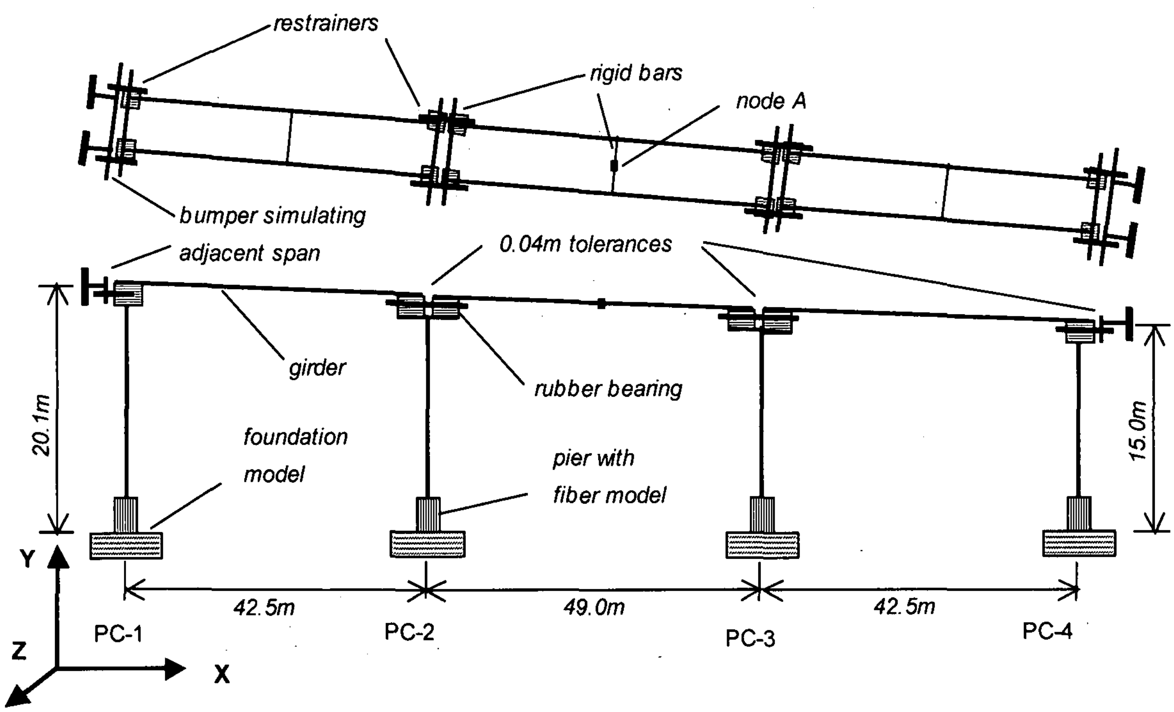

Fig. 3 Modeling of a three-span steel bridge

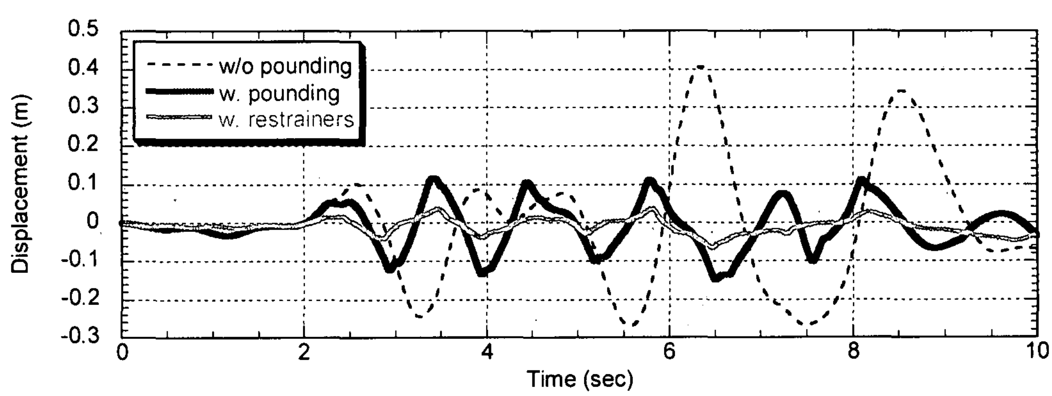

(a) Longitudinal displacements

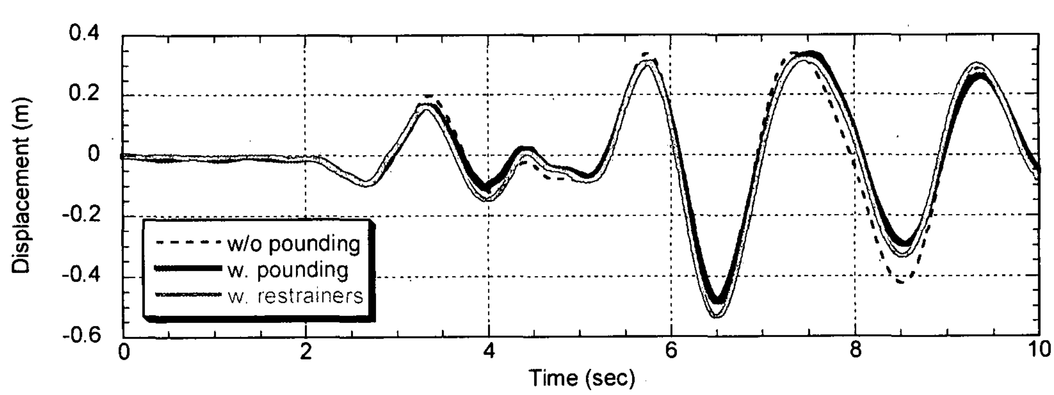

(b) Transversal displacements

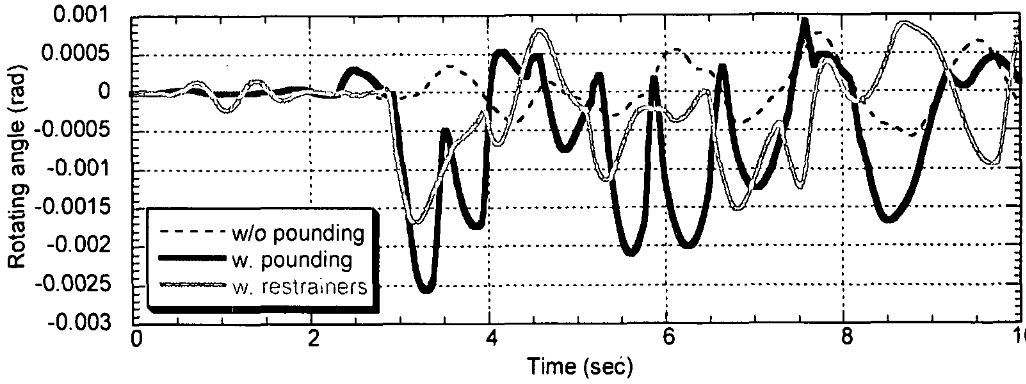

(c) Rotating angles

Fig. 4 Displacement comparisons of the mid span at node A

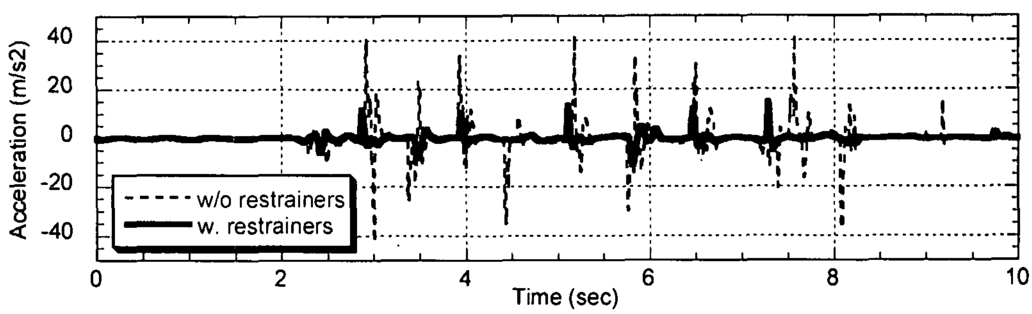

(a) Longitudinal accelerations

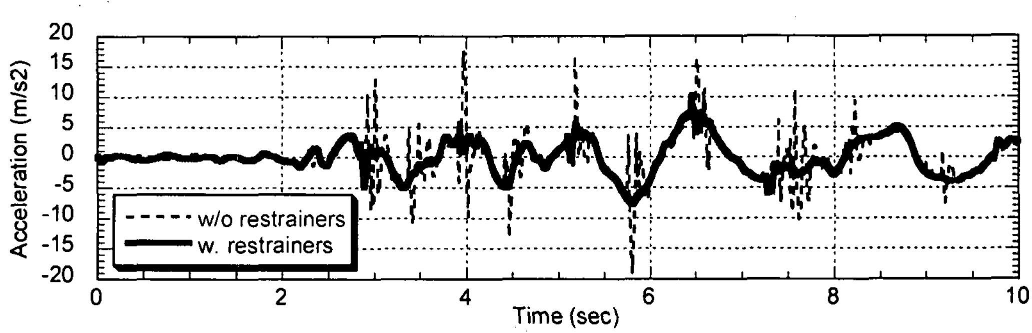

(b) Transversal accelerations

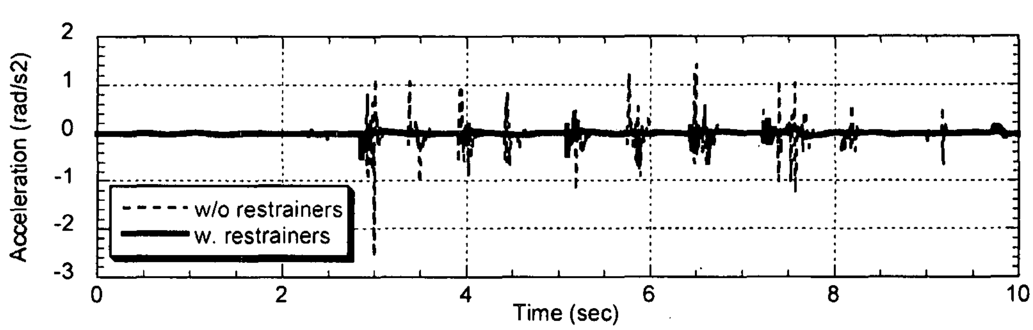

(c) Accelerations at rotating direction

Fig. 5 Accelerations at mid span at node A for the pounding case